Mechanical Properties of (poly(L-lactide-*co*-glycolide))-Based Fibers Coated with Hydroxyapatite Layer

Joanna Buczynska, Elzbieta Pamula, Stanislaw Blazewicz

Faculty of Materials Engineering and Ceramics, Department of Biomaterials, AGH University of Science and Technology, 30-059 Krakow, Poland

Received 15 July 2010; accepted 19 January 2011
DOI 10.1002/app.34189
Published online 12 April 2011 in Wiley Online Library (wileyonlinelibrary.com).

ABSTRACT: This article presents the results of the experimental study on manufacturing and mechanical evaluation of poly(L-lactide-*co*-glycolide) (PLGA)-based fibers modified with ceramic nanoparticles. Study was conducted to establish the effect of biomimetic formation of apatite layers on polymeric fibers on their mechanical properties. The tensile tests were performed to determine the influence of polymer crystallinity and the presence of hydroxyapatite nanoparticles (nanoHAp) on mechanical properties of PLGA fibers coated with hydroxyapatite (HAp) layer. HAp deposits on the surfaces of the fibers precipitated from simulated body fluid (SBF). Three types of fibers coated with HAp layers were compared in mechanical tests. The results indicated that by using a biomimetic fiber coating method the mechanical properties of the fibers are affected by their crystallinity. The nanoHAp modified polymer fibers after incubation in SBF were found to have a continuous HAp layer. The layer affected the mechanical behavior (force–strain function) of the fibers from nonlinear to linear, typical of ceramic materials. The tensile modulus of the fibers with a continuous layer was found to increase with the apatite layer thickness, whereas the tensile strength decreases. J Appl Polym Sci 121: 3702–3709, 2011

Key words: PLGA; nanocomposites; fibers; mechanical properties; apatite; biomedical application

INTRODUCTION

Polymer and ceramic materials applied separately do not display optimal mechanical and/or physico–chemical properties useful for medical applications. In such a case, combining the properties of both these materials seems to be a logical way aiming at manufacturing a composite material performing features of both polymeric materials and ceramics. At present, different ceramic materials are used for bone tissue regenerative and reconstructive processes, including pure calcium phosphates [tricalcium phosphate, hydroxyapatite (HAp)] as well as Bioglass-based composites.[1] HAp-based ceramics is currently widely used in the treatment of bone diseases.[2] Because of its bioactive behavior in living organism, the tissue is integrated with the implant through a newly formed apatite layer similar to that of a natural bone structure. Growth of a new apatite structure is a precondition for creation of the strong chemical bonds with the implant surface.[3,4] The HAp-based implants are characterized by their high biocompatibility with soft and hard tissues.[1–5] The biological properties and potential of PLA/HAp composites for bone surgery have been widely studied during the last decade.[6–9]

Many biomimetic methods for manufacturing of different kinds of phosphate layers on implant materials have been developed.[9–14] The concept of biomimetic layers is based on keeping a biomaterial (implant) in a simulated body fluid (SBF) containing the constituents similar to those existing during the formation of natural apatite.[11–18] The methods also involve chemical or physical modifications of polymers for deposition of inorganic phases.

An example of developed chemical methods are phosphorus-functionalized polymers in the form of films that were studied as substrates for ceramic layers. The films provide nucleation sites for the deposition of inorganic minerals such as HAp.[19] Another way is a direct addition of phosphate granules into poly(L-lactide), previously dissolved in a solvent followed by evaporation of the solvent. The obtained composite was verified successfully *in vivo* study.[7]

The design and manufacture of the biomaterials for bone surgery based on highly biocompatible HAp ceramics and resorbability of polymers seems to be a reasonable solution for production of medical implants, which may mimic the structure of natural

Correspondence to: S. Blazewicz (blazew@agh.edu.pl).
Contract grant sponsor: Ministry of Science and Higher Education, Statute Research, AGH University of Science and Technology (Krakow, Poland); contract grant number: 11.11.160.937.

bone. Moreover, the combination of ceramic components with biodegradable polymers allows for improvement of endurance polymers, adhesion of osteogenic cells, porosity, and ability for growth of osseous tissue.[4,14,15] Despite many scientific research dealing with deposition of biomimetic apatite on different polymer biomaterials both in the form of porous or fibrous scaffolds as well as in the form of films, the question arises how the polymer structure influences deposition process and resulting mechanical properties of a layered composite (layer/polymer). Particularly, considerations given to bioresorbable polymers-based fibrous materials are not broadly reviewed in the literature so far.

The aim of this study was to compare the poly(L-lactide-*co*-glycolide) (PLGA)-based fibers for biomimetic deposition of HAp from SBF. Two types of PLGA fibers were manufactured. The prepared fibers differed in crystallinity, diameters, and mechanical properties. The third type of the fibers was additionally modified with hydroxyapatite nanoparticles (nanoHAp). Susceptibility of these fibrous materials for manufacturing of a continuous apatite layer was analyzed.

MATERIALS AND METHODS

Materials production

The PLGA copolymer was obtained at the Centre of Polymer and Carbon Materials, Polish Academy of Science, Zabrze, Poland. Glycolide and L-lactide (Purac, Holland) was purified by recrystallization from dry ethyl acetate and dried in a vacuum furnace at room temperature. Zirconium(IV)acetylacetonate $Zr(acac)_4$ (Aldrich, Germany) was used as an initiator. Copolymerization was carried out in bulk with an initiator/monomer molar ratio of 1.25×10^{-3} at 100°C using a vacuum line for degassing and sealing of the ampoules, according to a method described previously.[20] Molar ratio of L-lactide to glycolide in the copolymer was found to be 84 : 16, as studied by ^{1}H-NMR (Varian Unity Inova). Number average molecular mass (Mn) and weight average molecular mass (Mw) of this copolymer were 190 kD and 320 kD, respectively, as studied by gel permeation chromatography (Physics SP8800). As ceramic additive, a nanoHAp powder produced according to a method described previously was used.[21] The average size of nanoHAp grains was about 200 nm, and crystallites size determined from X-ray diffraction was about 34 nm.[21]

Fibers manufacturing

The PGLA fibers were manufactured at the Technical University of Lodz, Department of Man-Made Fibres, Poland, using a laboratory scale-unit. A wet spinning technique from solution was applied to obtain a continuous fiber tow in the form of roving. The polymer solution (20% w/v) was prepared by dissolution of the PLGA copolymer in *N*,*N*-dimethylformamide (DMF). PLGA fibers modified with nanoHAp were spun from the solution containing 3 wt % HAp nanopowder. The spinning solution had an intrinsic viscosity of 1.46 assayed in DMF at room temperature. The spinning process was led in a solidification bath. Stretching process was carried out in a plastifying bath. A 240-hole spinning nozzle with holes of 0.08 mm in diameter was used. After solidification and stretching bath, the fibers roving passed through washing bath (in water) followed by drying process at room temperature.

Three types of fibers were prepared: pure PLGA fibers [high tensile strength (HTS)], pure PLGA fibers [low tensile strength (LTS)], and PLGA fibers containing 3 wt % nanoHAp (HAP). The LTS and HAP fibers were manufactured in a one-stage drawing process, whereas the HTS fibers were formed in a two-stage process of stretching, i.e., two stage distribution of deformations. In one-stage drawing process, the fibers tow was stretched in an aqueous plastification bath containing 35% DMF at 37°C with the draw ratio of 2.8. In a two-stage technique, the drawing process was conducted, first in a plastification bath followed by the second stage in a superheated steam at 135°C. The total draw ratio of two-stage drawing process was 5.7. After the drawing process, the fibers were rinsed off and dried at room temperature. Because of preparation of the fibers in different way, i.e., in one- and two-stage processes, their mechanical properties, crystalline structure, and diameters distinctly differed.

Apatite layer deposition

The SBF solution was prepared according to the procedure described elsewhere[14] by dissolving the following salts: 12.6 m*M* $NaHCO_3$, 1.5 m*M* Na_2SO_4, 7.5 m*M* $CaCl_2$, 4.5 m*M*, $MgCl_2 \cdot 6H_2O$, 13.2 m*M* KCl, 3.0 m*M* K_2HPO_4, and 410.4 m*M* NaCl in ultra high quality water (UHQ-water) produced in Purelab apparatus (Elga, UK). The concentrations of salts in SBF were thrice higher than those occurred in natural body fluid. The reason of the use of such concentration of salts was to accelerate the deposition process of the apatite on the fiber surface and to avoid the degradation process during this procedure, which could lead to lowering mechanical proprieties of the fibers. The SBF solution was buffered with tris(hydroxymetylo)aminomethane and hydrochloric acid to reach the pH of 7.28.

Hydroxypatite layer was deposited on two types of the samples: the first one for physico–chemical

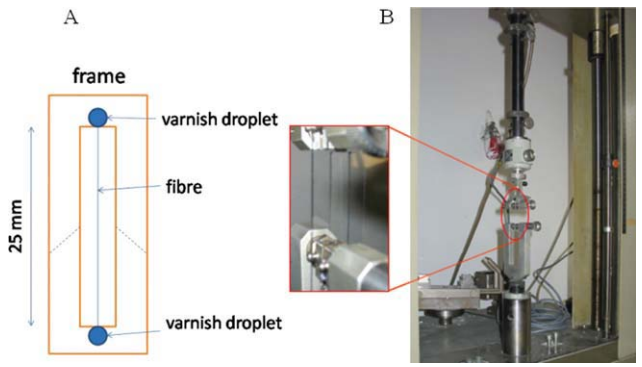

Figure 1 A: Schematic representation of the frame for tensile tests of individual fibers; (B) method of mounting the frame with the fibers in the grips of universal testing machine. [Color figure can be viewed in the online issue, which is available at wileyonlinelibrary.com.]

evaluations, and the second one for mechanical tests. In the first case, weighed amount of fibers (500 mg) in the form of bundles was placed in plastic vials containing 100 mL of SBF in an incubator at 37°C for 5, 10, and 15 days. For tensile tests, individual fibers were collected from the bundles and glued with the use of nail varnish to plastic frames prepared from a photocopy foil (Staedler, Germany). Schematic representation of the frame with the glued fiber is presented in Figure 1(A). Thirty-five frames with the fibers of each type were placed in plastic vials containing 100 mL of SBF and stored in an incubator at 37°C for 5, 10, and 15 days. After a desired period of time, the samples were collected, rinsed thrice in UHQ-water, and dried in a vacuum chamber at 25°C for 24 h.

Characterization methods

The surface morphology of the fibers was studied by means of a scanning electron microscope (SEM, JSM-5400, JEOL, Japan) under magnifications of 1000 and 2000 times. Before analysis, the samples were coated with a thin carbon layer to make them conductible. Elemental composition of the samples was studied by energy dispersive X-ray (EDX) spectroscopy (Link AN 10000, UK).

Fourier transform infrared (FTIR) spectra of the fibers were made using FTS-60V Digilab Division spectrometer, BIORAD type. The fibers were crushed and mixed with KBr to form pallets and transmission spectra were recorded with a resolution of 4 cm^{-1} by averaging of 256 scans for each spectrum.

The structure and crystallinity of phosphate deposits and polymer fibers were investigated by X-ray powder diffraction (XRD) using diffractometer Richard Seifert and Co. XRD7. Before the analysis, the fibers were crushed and powdered. Angle measurements (2θ) were conducted in the range from 5 to 70 degrees. The apparent crystallite sizes of PLGA and HAp were calculated from the Sherrer equation for the peaks at 17 degrees and 32 degrees, respectively.

The original single fibers without and with apatite layers were investigated using tensile tests to determine their mechanical properties. The diameters of each individual fiber were determined before tensile tests by using an optical microscope. The evaluation of static mechanical properties (tensile strength and modulus, strain to rupture) was made using ZWICK 1435 testing machine, PC controlled by TestXpert v.8.1 software (Zwick, Germany). The frames with the fibers were mounted in the grips of the testing machine as shown in Figure 1(B). Then, the frames were gently cut with the scissors in the places shown as dashed lines in Figure 1(A). The crosshead speed of the testing machine was 2 mm/min. Because of nonlinear force-elongation relationship, the tensile modulus was determined from the slope of the function at its initial run, i.e., in the range of 0.005–0.01 N. For each type of the fibers, 35 individual filaments were measured. The results are presented as averages and standard deviations. Statistical comparisons between the groups of samples were made with Student's *t*-test, with a chosen level of significance of $P \leq 0.05$. The $P \leq 0.05$ values were considered significant.

RESULTS AND DISCUSSION

Table I gathers the base parameters of the fibers used in the study before incubation process determined in tensile tests. As the HTS fibers were obtained in two-stage drawing process, their mean diameter is much smaller then diameter of the fibers obtained in one-stage process. Because of improved orientation of the supramolecular polymer structure during two-step drawing process, the resulting strength properties of the HTS fibers are significantly higher in comparison with HAP and HTS fibers. On the contrary, comparison between both types of fibers spun in one-stage process shows a

TABLE I
Properties of PLGA Fibers

	HAP	HTS	LTS
Diameter (μm)	29.0 ± 3.2	16.9 ± 1.4	27.3 ± 1.9
Strength (MPa)	31.4 ± 1.8	62.0 ± 4.0	24.8 ± 1.8
Young's modulus (GPa)	1.1 ± 0.1	1.2 ± 0.1	0.8 ± 0.1
Strain to failure (%)	7.6 ± 0.6	12.6 ± 0.8	7.8 ± 0.5
Crystallite size (nm)	1.25 34[a]	7.45	0.92

Averages ± SD.
[a] Size of HAp crystallites in this fiber.[21]

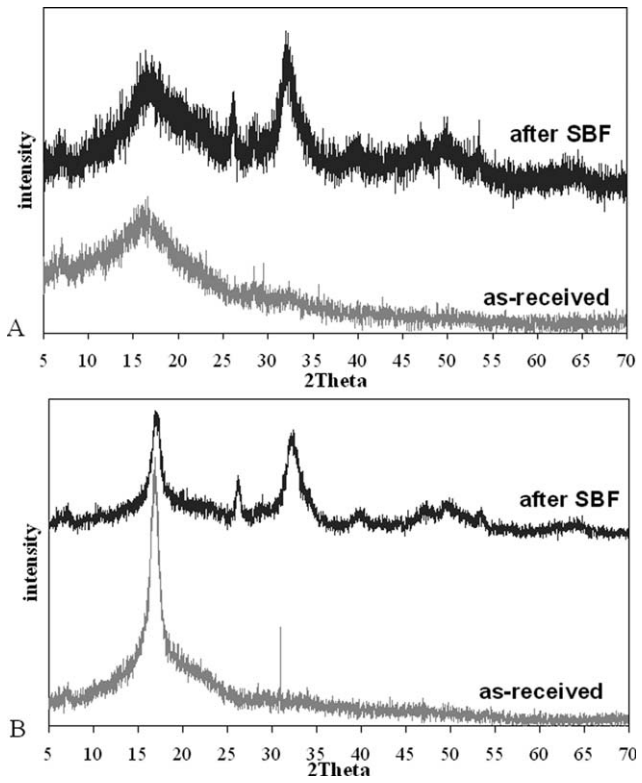

Figure 2 XRD diffractograms of PLGA fibers: (A) HAP fibers and (B) HTS before and after incubation in SBF for 15 days.

distinct increase in mechanical properties for the fibers containing HAp nanoparticles. Specifically, the HAP fibers show about 35% increase in Young's modulus and a 25% increase in the tensile strength as compared with the LTS fibers. This a substantial improvement in mechanical properties of the HAp-modified fibers can be explained in view of reinforcement of pure polymer matrix due to presence of ceramic nanocomponent.

Figure 2 presents XRD diffractograms of HAP and HTS fibers prior and after soaking in SBF for 15 days. The diffractograms of as-received HAP fibers [Fig. 2(A)] and LTS fibers (data not presented here) show a single broad peak at about 17°. A narrower and much stronger peak corresponds to the HTS fibers that were obtained in the two-stage process of stretching fibers [Fig. 2(B)]. Such a process allows for preparation of the fibers with a more ordered crystalline structure. The apparent crystallite size for these fibers was 7.45 nm, whereas for the LTS fibers this parameter was about 0.92 nm (Table I). The reason of higher crystallinity of HTS fibers was a higher total deformation during their drawing process. The crystallinity of HAP fibers is a slightly higher (statistical significance $P \leq 0.05$) compared with that for LTS fibers. This observation suggests that the incorporation of ceramic nanoparticles into the PLGA copolymer solution slightly affects the crystalline arrangement at the stage of fibers drawing. After incubation in SBF, new peaks originating from HAp are visible at 32° and near 26° (2θ). The determined crystallite size of HAp deposited on the surface of fibers is about 20 nm.

Typical FTIR spectra of pure PGLA fibers before and after incubation in SBF are shown in Figure 3.

The spectrum of pure PGLA fibers shows the band at 1750 cm^{-1}, characteristic for the stretching mode attributed to C=O groups as well as the bands at 1456 cm^{-1} and at 1385 cm^{-1} brought about the deformation vibration of CH_3 groups of PLGA. In the spectrum of fibers after incubation in SBF, besides the bands specified above, new bands appear that are characteristic for the phosphate groups occurred in the HAp structure. The spectra of these fibers contain the bands originating from stretching vibrations of P—O phosphate groups at about 1040 cm^{-1} (arrow). The spectra also display the bands at 563 cm^{-1} and 605 cm^{-1} brought about by the bending mode of phosphate groups (arrow).

Morphological documentations of the ceramic deposits crystallized on the surfaces of the fibers evaluated with the use of SEM are gathered in Figure 4. After 5-day incubation, the separated spherical deposits on the surface of LTS and HTS fibers were observed [Fig. 4(D,G)]. On the contrary, the surface of HAP fibers was entirely covered with a thin ceramic layer [Fig. 4(A)]. EDX analysis of the deposits showed that Ca/P ratio was in the range of 1.5–1.7, which is close to that in HAp. After a longer time of incubation (15 days), the layer formed on HTS fibers was discontinuous and revealed large size defects and detached fragments of the layer [Fig. 4(F)]. It indicates that adhesion between the layer and the surface is rather weak. A prolonged incubation of HAP and LTS fibers led to further apatite growth accompanied by an increase in the fiber diameter (Fig. 5). On the contrary, the mean diameter of HTS fibers after 5 days does not change,

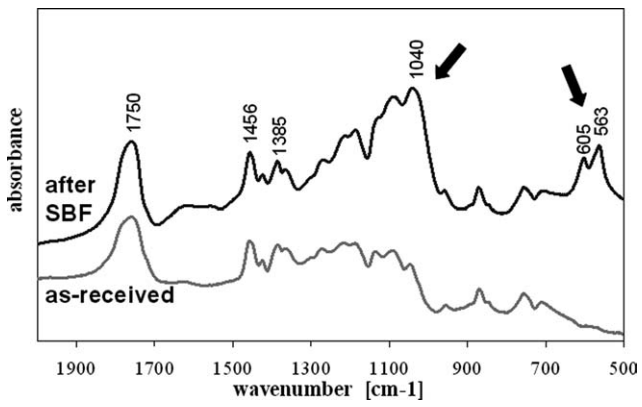

Figure 3 FTIR spectra of LTS fibers before and after incubation in SBF for 15 days.

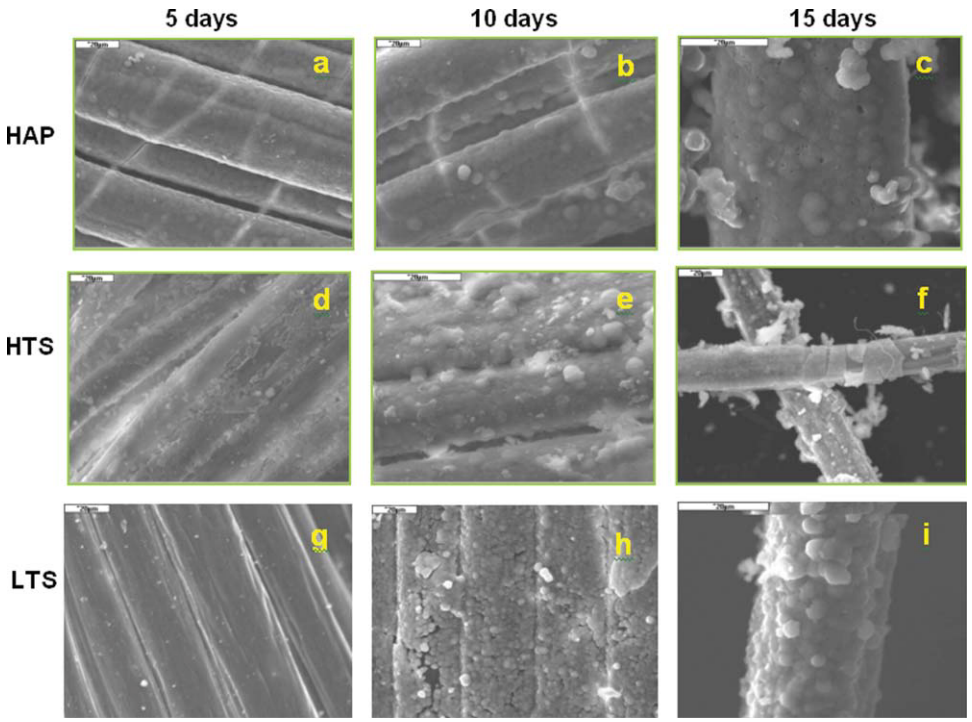

Figure 4 Surface morphology of PLGA fibers: HAP (A–C), HTS (D–F), and LTS (G–I) after 5 days (A, D, G), 10 days (B, E, H), and 15 days (C, F, I) of incubation in SBF; scanning electron microscope, original magnification ×1000 and ×2000. [Color figure can be viewed in the online issue, which is available at wileyonlinelibrary.com.]

whereas after longer time (15 days) it shows a tendency to decrease, with statistical significance $P \leq 0.001$ as compared with the samples received after 10-day incubation. As the fiber/matrix interfacial interaction is low, the thicker layer deposited on the HTS surface has a tendency for splitting out; therefore, the mean diameter for those fibers reaches almost the value of the pristine fibers (a denuded original surface is seen) [Fig. 4(F)].

The room temperature tensile properties of various fibers subjected to incubation in SBF are shown in Figures 6–8.

Figure 6 shows the tensile strength of three types of fibers as a function of incubation time in SBF. The LTS and HAP fibers show nearly identical changes, and after the 15-day incubation, a significant decrease in strength of both fibers is observed. Much smaller changes (less than 15%) are observed for HTS fibers. Similar tendency is observed for variation of strain to failure (Fig. 7). Both types of fibers (LTS and HAP) after deposition of ceramic layer display the strain to failure below 1%, which corresponds to typical values found for ceramic materials. On the contrary, the fibers having better mechanical

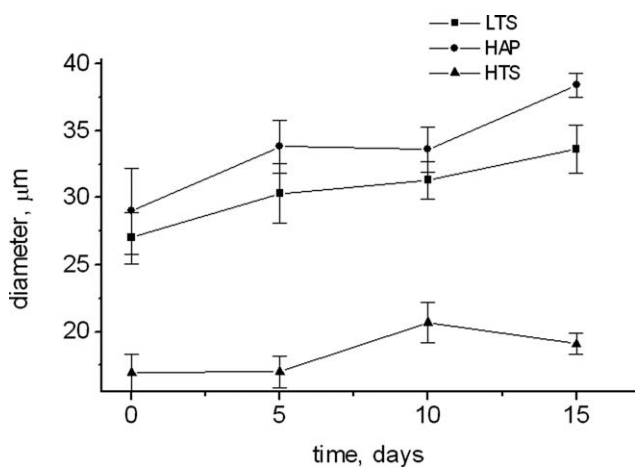

Figure 5 Variation of mean diameters of PLGA fibers as a function of incubation time in SBF.

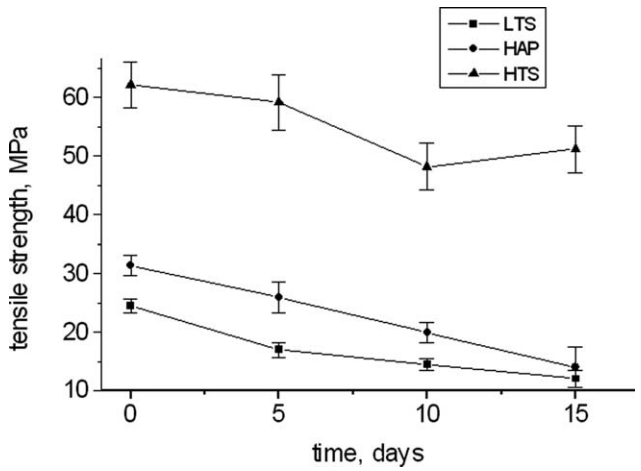

Figure 6 Variation of tensile strength of PLGA fibers as a function of incubation time in SBF.

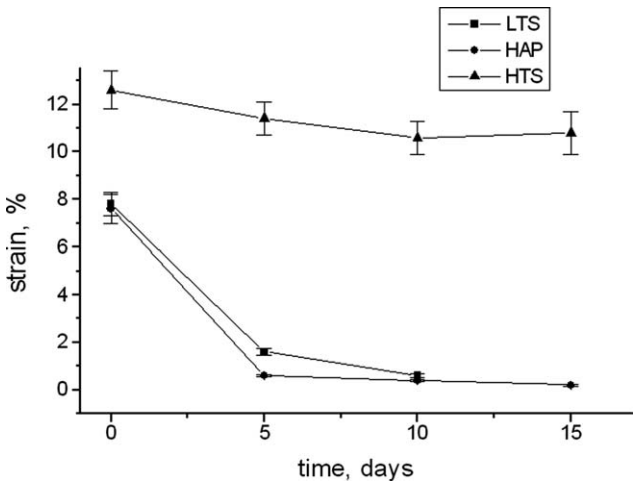

Figure 7 Variation of strain to failure of PLGA fibers as a function of incubation time in SBF.

properties and a better structural ordering (HTS) show almost comparable values of the strains before and after incubation in SBF.

The HTS fibers show a particular dependence of the tensile modulus of the fibers before and after incubation (Fig. 8). After 10-day incubation, a maximum of the fiber modulus is observed, whereas after 15-day incubation the fiber with ceramic layer reaches the values of original pure fiber (without layer). A possible explanation of such a behavior provides microphotographs of the fiber surface shown earlier [Fig. 4(F)]. A prolonged incubation of HTS fibers led to partial detaching the layer. Because such a fiber is only partially covered with the ceramic layer, and its adhesion is very weak, a force–strain run during tensile loading is the same as for pure HTS fiber (without layer) [Fig. 9(A,B)]. Figure 9(A,B) represents a typical relationship force–strain in the tensile test for the fibers before and after incubation in SBF. These results are useful in demonstrating and comparing the mechanical characteristics of the original PGLA fibers, composite fibers, and the fibers coated with HAp layers. The figures perform the changes of dependency profiles between the force and strain for pure fiber and the fiber coated with HAp. It is evident that the most significant changes are observed for graphs of the HAP fibers [Fig. 9(A)]. After 15 days of incubation, the graph for this fiber is linear within the whole range of elongation. Such a dependence confirms the brittle behavior of the formed layer, typical for the ceramic materials. As a consequence of the change of this dependency from nonlinear into linear one, a total strain to failure decreases. The determined values of Young's modulus for these fibers are clearly higher than those obtained for the fibers without coating. An average diameter of these fibers after 15-day incubation is about 37 μm, which indicates that the fiber is confined with about 4-μm-thick apatite layer. A simple calculation of volume fraction of apatite layer related to the total volume of composite fiber (fiber plus layer) gives the value of 39%. For two phase composite system, the simple rule of mixtures for tensile modulus can be written, as follows: $E_c = E_f V_f + E_l V_l$, where E_c is a tensile modulus of composite fiber, $E_f V_f$ and $E_l V_l$ denote contributions to tensile modulus of pure HAP fibers, and apatite layer, respectively. As E_f is 1.1 GPa and $V_f = 0.39$ (Table I), and E_l for typical synthetic apatites ranges from 35 to 110 GPa, it can be further written that, $E_f V_f < E_l V_l$.[22] In other words, the tensile modulus is largely dependent upon the apatite layer confining the HAP fiber, and the contribution of pure HAP fiber (without layer) in total tensile modulus of the composite fiber can be neglected. Thus, the resulting force–strain curve for this fiber is entirely linear [Fig. 9(Ac)].

On the contrary, the dependences for HTS fibers do not change their shape and after 15-day incubation sustain their nonlinear character (9B). For LTS fibers, the dependency (not shown here) is similar to that of the HAP fibers.

Figure 10 presents the amount of HAp deposited on the fiber unit surface as a function of incubation time. The data were calculated on the assumption of diameter increase as a function of soaking in SBF due to deposition of HAp of known density (3.12 g/cm^3). As it results from this figure, the apatite deposition process is more intensive on the surface of the HAP fibers. These fibers contain HAp grains in the volume and on their surface creating the crystallization centers that accelerate the formation of apatite. In the case of HTS fibers, the deposition of apatite after 5 days is very low and is effective till day 10 of the experiment. Prolongation of this process does not lead to the increase of depositing HAp. The HTS

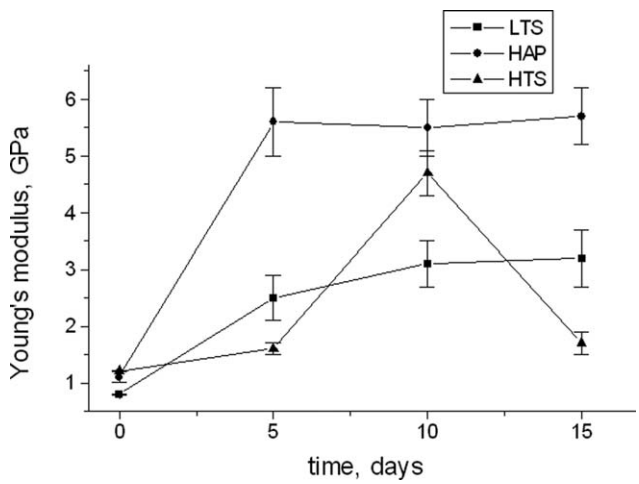

Figure 8 Variation of Young's modulus of PLGA fibers as a function of incubation time in SBF.

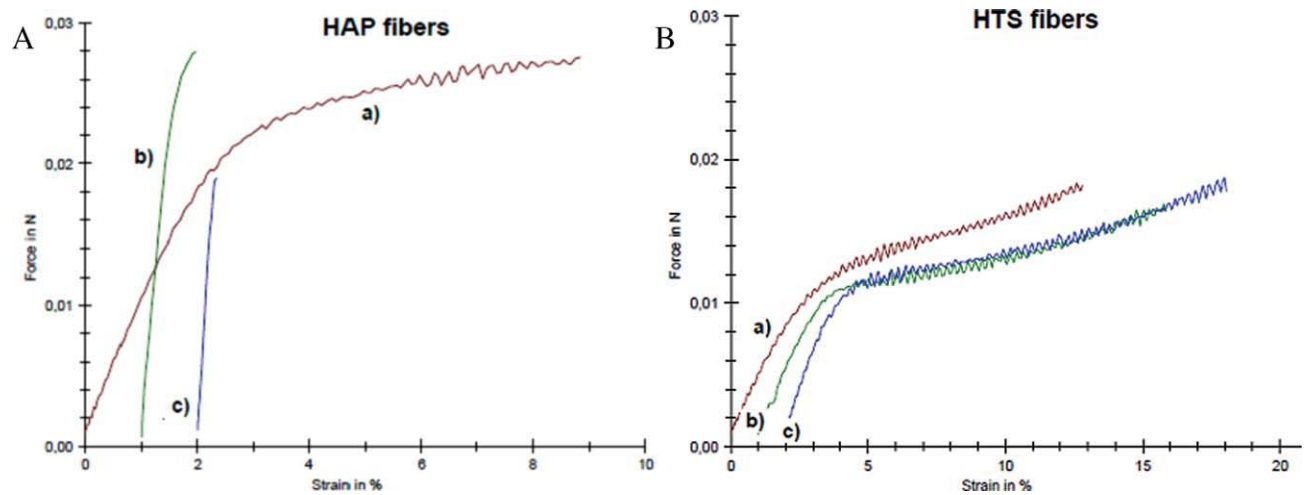

Figure 9 Force–strain relationships of PLGA fibers [HAP (A) and HTS (B)] before and after different period of time of incubation in SBF; (a) as received, (b) after 5 days, (c) after 15 days. [Color figure can be viewed in the online issue, which is available at wileyonlinelibrary.com.]

fibers differ from HAP fibers in mechanical properties and crystallinity of the polymer. According to Table I, the apparent crystallite size of these fibers is significantly higher in comparison with HAP and LTS fibers. It is very probable that crystalline structure of the surface of these fibers may play a role in a diverse process of the apatite crystallization. This fact results both from the estimated mass of apatite related to the surface unit as well as from morphology of the deposits. HTS fibers display a less defected and a better ordered surface (higher crystallinity) and posses a lower surface energy, which may influence in lowering the rate of the crystallization process. It is worthy to note that the changes in apatite mass on the HTS fiber surface shown in Figure 10 are in a good agreement with the changes of Young's modulus (Fig. 8) and fibers diameter (Fig. 5). The reason of the observed inhibition of apatite deposition is that the layer does not adhere properly to the fiber surface and, therefore, the loose fragments fall from the surface. This effect is also visible in the microphotograph [Fig. 4(F)]. The microscopic observations indicate that the apatite deposits created on the HTS fiber surface are rather loosely attached to the surface and do not affect the force–strain relationship of these fibers. The HAP fibers create a continuous compact layer, and after a longer period of incubation, the process of growth leads to durable interconnections within the bundle of fibers. The presence of HAp embedding into the near surface region of the fibers influences the adhesion of the formed layer to the polymer surface and alters their mechanical characteristics. The results indicate that exposure of the PLGA fibers to incubation in a concentrated SBF solution leads to significant changes in their mechanical properties. However, a good interfacial bonding or interaction between fiber/apatite layer can be obtained only for the low crystalline fibers (low crystallite size) or for the fibers containing ceramic particles located on their surface.

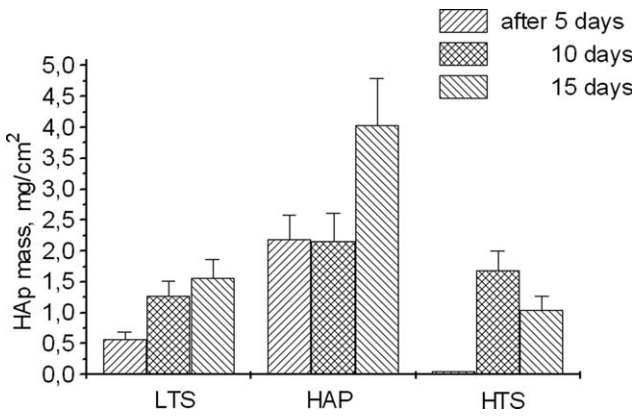

Figure 10 Average mass of hydroxyapatite deposited on PLGA fibers surface after incubation in SBF.

CONCLUSIONS

Biomimetic modification of PLGA fibers by coating them with apatite layer was investigated. It was shown that by incubation of PLGA fibers in the concentrated SBF a continuous coating can be obtained. The structure of the formed coatings analyzed by FTIR and XRD indicates that HAp deposit consists of 20 nm crystallites. Continuous ceramic layers were formed on the fiber surface modified with nanoHAp particles and on a low crystalline fiber surface. On the contrary, the surface of the pure PLGA fibers obtained in a two-stage spinning process was coated with discontinuous, fractured layers and showed a weak bonding with the fiber surface.

It is speculated that the reason is a higher crystallinity of these fibers. A distinct difference in the deposit morphology was observed for the fibers having nanoHAp particles embedded into the fiber. Because of continuous layer formed on the surface of the fiber, its mechanical characteristics that are initially nonlinear alter to entirely linear, which is typical of ceramic materials. For the fibers coated with thick layers (10–15 days of incubation), the tensile stress is transferred mainly by the ceramic phase. An optimum time for deposition of HAp layers was about 10 days. The most effective increase of the ceramic deposit was noted for the fibers initially modified with nanoHAp particles. It means that the presence of HAp in PLGA structure accelerates biomimetic crystallization of calcium phosphate from SBF. Such a mechanism may also be expected *in vivo* environment.

References

1. Chevalier, J.; Gremillard, L. J Eur Ceram Soc 2009, 29, 1245.
2. Hench, L. Biomaterials 1998, 19, 1419.
3. Billote, W. G. In Biomaterials: Principles and Applications; Park, J. B., Bronzino, J. D., Eds.; CRC Press: Boca Raton, 2003; pp 27–39.
4. Ma, P. X. Adv Drug Deliv Rev 2008, 60, 184.
5. Liao, J.; Guo, X.; Nelson, D.; Kasper, F. K.; Mikos, A. G. Acta Biomater 2010, 6, 2386.
6. Ignjatovic, N.; Tomic, S.; Dakic, M.; Miljkovic, M.; Plavsic, M.; Uskokovic, D. Biomaterials 1999, 20, 809.
7. Ignjatovic, N.; Savic, H.; Najman, S. Biomaterials 2001, 22, 571.
8. Gay, S.; Arostegui, S.; Lemaitre, J. Mater Sci Eng 2009, C29, 172.
9. Zhang, P.; Hong, Z.; Yu, T. Biomaterials 2009, 30, 58.
10. Liao, S. S.; Cui, F. Z.; Zang, W.; Feng, Q. L. J Biomed Mater Res B 2004, 69B, 158.
11. Kawashita, M.; Nakao, M.; Minoda, M.; Kim, H. M.; Beppu, T.; Miyamoto, T.; Kokubo, T.; Nakanura, T. Biomaterials 2003, 24, 2477.
12. Takeuchi, A.; Ohtsuki, C.; Miyazaki, T.; Tanaka, H.; Yamazaki, M.; Tanihara, M. J Biomed Mater Res A 2003, 65A, 283.
13. Li, J.; Lu, X. L.; Zheng, Y. F. Appl Surf Sci 2008, 255, 494.
14. Douglas, T.; Pamula, E.; Hauk, D.; Wiltfang, J.; Sivananthan, S.; Sherry, E.; Warnke, P. H. J Mater Sci Mater Med 2009, 20, 1909.
15. Kretlow, J. D.; Mikos, A. G. Tissue Eng 2007, 13, 927.
16. Murphy, W. L.; Kohn, D. H.; Mooney, D. J. J Biomed Mater Res 2000, 50, 50.
17. Landi, E.; Tampieri, A.; Celotti, G.; Langenati, R.; Sandri, M.; Sprio, S. Biomaterials 2005, 26, 2835.
18. Kokubo, T.; Takadama, H. Biomaterials. 2006, 27, 2907.
19. Jin, S.; Gonsalves, K. E. J Mater Sci Mater Med 1999, 10, 363.
20. Dobrzynski, P.; Kasperczyk, J.; Janeczek, H.; Bero, M. Macromolecules 2001, 34, 5090.
21. Haberko, K.; Bucko, M.; Brzezinska-Miecznik, J.; Haberko, M.; Mozgawa, W.; Panz, T.; Pyda, A.; Zarebski, J. J Eur Ceram Soc 2006, 26, 537.
22. Suchanek, W.; Yoshimura, M. J Mater Res 1998, 13, 94.